2P2-15

Numerical analysis of linear wave propagation in the atmosphere with temperature gradient for Mach cutoff reproduction

マッハカットオフ再現を目指した温度勾配を持つ大気中の線形音波伝搬解析

Takao Tsuchiya[1,2†], Masashi Kanamori[2], and Takashi Takahashi[2] ([1]Faculty of Science and Engineering, Doshisha Univ., [2]JAXA)
土屋隆生 [1,2†]，金森正史 [2]，高橋　孝 [2] ([1] 同志社大・理工，[2]JAXA)

1. Introduction

The development of the next generation supersonic transport (SST) is being pursued at a rapid pace. However, there is a problem of sonic boom in commercializing SST. The prediction of sonic boom propagation is an important issue since the sonic boom can not be completely suppressed.

In the prediction of sonic boom propagation, a combination method of computational fluid dynamics (CFD) and the augmented Burgers equation has been applied [1]. This is effective when the sound ray reaches the ground surface, but it can not be applied when Mach cutoff occurs. Mach cutoff is a phenomenon in which the sound rays escape to the sky by drawing an arc due to the existence of the temperature gradient when the aircraft cruises at a speed in the vicinity of $M = 1$, as shown in Fig. 1.

In this paper, numerical analysis of the two-dimensional linear wave propagation in the atmosphere with temperature gradient is peformed in order to reproduce the Mach cutoff and predict the evanescent wave below the caustic. The compact explicit finite-difference time-domain (CE-FDTD) method [2, 3] is applied to analysis. A sound source model by phased array is proposed to simulate shock waves radiated obliquely from the aircraft. Some demonstrations are performed on the reproduction of Mach cutoff evanescent waves.

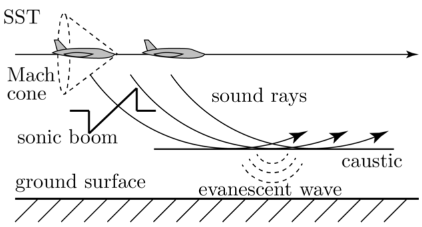

Fig.1　Mach cutoff and caustic.

2. Theory

In the CE-FDTD method, 2-D wave equation is discretized considering not only the axis directions but also the face diagonal directions as [2]

$$\delta_t^2 p_{i,j}^n = \chi^2[(\delta_x^2 + \delta_z^2) + b\delta_x^2\delta_z^2]p_{i,j}^n \qquad (1)$$

where $p_{i,j}^n$ represents the sound pressure at the grid point $(x, z) = (i\Delta, j\Delta)$ at time $t = n\Delta t$, Δt is time step, $\chi = c(z)\Delta t/\Delta$ is the Courant number, $c(z)$ is the sound speed at height z, b denotes numerical parameter. The grid intervals of *x*-, and *z*-directions are assumed to be all the same, Δ. δ^2 is an operator on the central finite difference.

In order to simulate sound radiation in an oblique direction, a phased array source is proposed as shown in Fig. 2. The phased array consists of driving sources located at grid points and delay elements. The radiation direction is controlled by delay time of each element. The delay time of the *i*-th element (grid point) is given as

$$\tau = i\Delta/\mathrm{v} \qquad (2)$$

where v is flight speed.

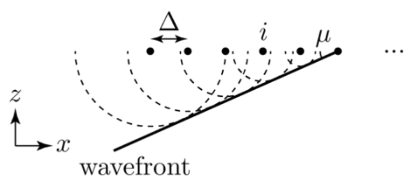

Fig.2　A phased array source.

3. Numerical experiments

The medium is assumed to be the standard atmosphere whose sound speed is given as [4]

$$c(z) = c_0 + g_1 z + g_2 z^2 \qquad (3)$$

where c_0 is sound speed at ground surface 340.3 m/s, $g_1 = -3.83\times10^{-3}$ 1/s, and $g_2 = -2.54\times 10^{-8}$ 1/(ms). In this paper, it is assumed that the equation (3) can be applied even for altitude of 11 km or more for simplicity. The grid size is Δ=0.5 m, the time step is Δt=1.47 ms, so the Courant number χ is 1 at maximum sound speed c_0. The region is divided into 260,000×30,000 FDTD cells. The boundary condition for the ground surface is rigid and the other is Higdon's second order absorbing boundary. The sound source is a phased array with a length of 129 km starting from the

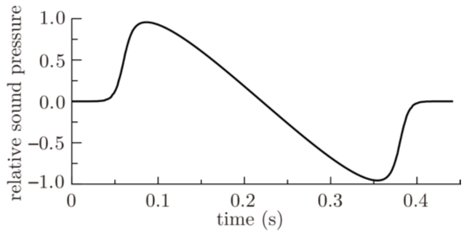

Fig.3 Radiated pulse.

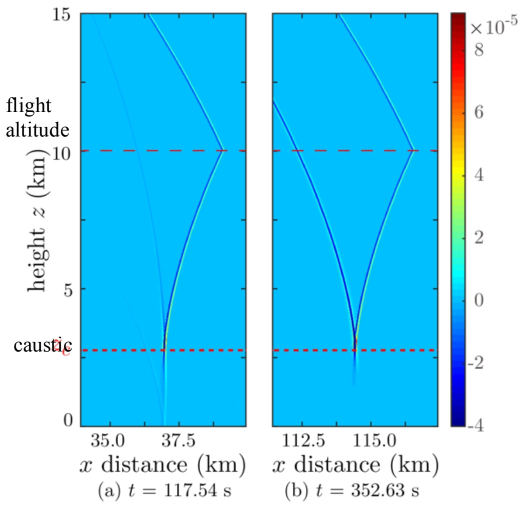

Fig.4 Sound pressure distributions.

position (1, 10) km. The flight speed is $M = 1.1$ ($v = 329.38$ m/s) in which Mach cutoff occurs at flight altitude of 10 km. A single pulse of a shock wave shape with a pulse width of 0.35 s shown in Fig. 3 is radiated from the phased array.

Figure 4 shows the calculated sound pressure distributions at (a) $t = 117.54$ s and (b) $t = 352.63$s. In this case, the caustic altitude is 2.791 km. It is confirmed that sound waves are radiated obliquely from the aircraft. The Mach angle measured from the figure is 66 degrees, which almost agrees with the theoretical value (65.38 degrees). In Fig. 4 (a), the reflection from caustic is partially confirmed, but the caustic has not been completely formed and the Mach cutoff does not occur yet. On the other hand, in Fig. (b), the caustic is sufficiently formed, and Mach cutoff including total reflection is observed. Some waves seep out as the evanescent wave below the caustic.

Figure 5 shows the expanded sound pressure distributions in the vicinity of caustic at $t = 352.63$ s. Figure (a) shows the result of CE-FDTD method and (b) shows the result of CFD [5]. In the result of the CE-FDTD method, a stripe pattern appears behind the sound wave due to numerical dispersion error. Except for the numerical dispersion error, the two results agree well and the evanescent waves are also expressed. It is confirmed that the Mach cutoff can be reproduced by the CE-FDTD method.

Figure 6 shows the sound pressure waveforms

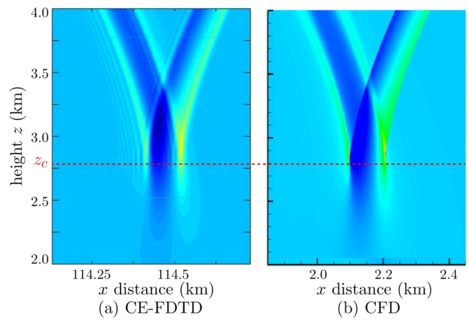

Fig.5 Expanded distributions in the vicinity of caustic.

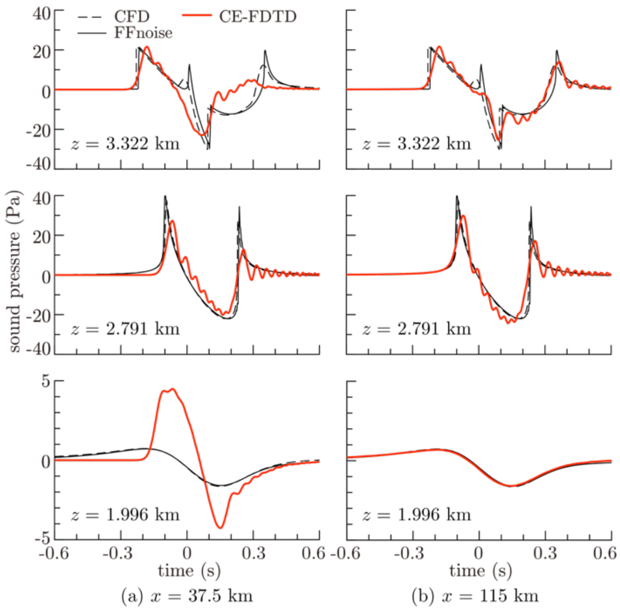

Fig.6 Sound pressure waveforms.

at various distances and altitudes. In the figures, the dashed lines indicate the results by CFD, the fine lines FFnoise [6], and the bold red lines CE-FDTD method. Except for the numerical dispersion error, the result of the CE-FDTD method is in good agreement with the other methods at x=115 km even linear analysis. On the other hand, at x=37.5 km, no caustic has yet been formed, so it does not agree with the results by other methods. For accurate analysis, a sufficiently long propagation distance is required for caustic formation. It is suggested that nonlinear analysis is not always required for the analysis of evanescent waves below caustic.

References

1. M. Kanamori, et al.: AIAA J., **56** (2018) 2743.
2. K. Kowalczyk et al.: IEEE Trans. Audio Speech and Lang. Process., **18** (2010) 78.
3. T. Ishii, T. Tsuchiya, and K. Okubo: Jpn. J. Appl. Phys., **52** (2013) 07HC11.
4. ISO: Standard Atmosphere, ISO 2533:1975.
5. R. Yamashita, et al.: Trans. Jpn. Soc. Aero. Space Sci., **58** (2015) 327.
6. M. Kanamori, et al.: AIAA J., **55** (2017) 2029.